JOURNAL OF VIROLOGY, Dec. 1995, p. 7489–7496 Vol. 69, No. 12
0022-538X/95/$04.00+0
Copyright © 1995, American Society for Microbiology

The Mismatched Nucleotides in the 5′-Terminal Hairpin of Minute Virus of Mice Are Required for Efficient Viral DNA Replication

EITHNE COSTELLO,[1] ROLAND SAHLI,[2] BERNHARD HIRT,[1] AND PETER BEARD[1]*

Swiss Institute for Experimental Cancer Research, 1066 Epalinges,[1] and Institute of Microbiology, Centre Hospitalier Universitaire Vaudois, 1011 Lausanne,[2] Switzerland

Received 17 July 1995/Accepted 21 August 1995

The 5′-terminal sequence in the DNA of the parvovirus minute virus of mice (MVM) is a palindrome. It can form a hairpin, the stem of which is entirely base-paired except for three consecutive unpaired nucleotides which form a bubble. Since this structure is well conserved among different parvoviruses, we examined its importance for viral replication by generating MVM mutants with alterations in this region. A clone of MVMp DNA which contained the entire 3′ end and more than half of the 5′ palindrome was made. Although it lacked the sequence information to form a wild-type bubble, this DNA was infectious. On transfection into A9 fibroblasts, it gave rise to a virus (MVMs) which had a bubble in its 5′ palindrome. The bubble consisted of four mismatched nucleotides in the same location as the unpaired nucleotides of the wild-type palindrome. Apparently, neighboring plasmid sequences were incorporated into the viral DNA, enabling formation of the mismatch. This observation suggested that a bubble is critical for growth of MVM but that its sequence is not. To find out whether MVM lacking a bubble in the 5′ palindrome is viable, we made a second clone in which the plasmid sequences incorporated in MVMs were removed. Transfection of this DNA gave rise to a virus (MVMx) in which the nucleotides unpaired in the wild-type hairpin are now fully base-paired. Although MVMx can be propagated, it is defective in comparison with wild-type MVMp; it exhibited about a 50-fold-lower ratio of plaque-forming units to DNA content. In mixed infections, MVMp consistently outgrew the bubbleless MVMx. The rate of accumulation of DNA replication intermediates was lower for MVMx than for the wild-type virus. Quantitative analysis of the 5′ termini of replicative form DNA suggested that the ability of MVMx to convert hairpin 5′ termini to extended termini is impaired. In contrast, the virus with the altered bubble, MVMs, behaved like the wild-type MVMp in all the assays. We conclude that MVM lacking a bubble in its 5′-terminal DNA hairpin is less infectious than and has a selective disadvantage compared with wild-type MVM. The nucleotide sequence of the bubble is not critical. We provide evidence that the presence of a bubble is necessary for efficient viral DNA replication.

The parvovirus minute virus of mice (MVM) has a linear single-stranded DNA genome 5,146 nucleotides in length, with short double-stranded hairpin structures at the 3′ and 5′ termini. The virus replicates its DNA by a mechanism called rolling-hairpin replication, for which it is dependent on the host cell undergoing the S phase of the cell cycle. The 3′-terminal hairpin serves as a primer for synthesis of the first complementary strand, giving rise to a duplex monomeric replicative form (mRF) DNA. An 83-kDa virally encoded protein (NS-1) introduces single-stranded site-specific nicks, allowing the production of replication intermediates which are dimeric and tetrameric forms of the unit-length genome. From these intermediates, single-stranded DNA is produced for encapsidation (for a review, see reference 3).

Studies of MVM DNA replication show the terminal hairpins to be essential. By analyzing viruses with incomplete genomes, Faust and Ward (13) demonstrated that all the critical recognition sites necessary for the replication of MVM DNA are contained within the hairpins. Moreover, cloned fragments representing right-end to right-end (viral 5′ to 5′) junctions from tetrameric RF DNA (7, 9) and left-end to left-end (viral 3′ to 3′) junctions from dimeric RF DNA (8, 9, 17) serve as replication origins in the presence of NS-1, confirming that the hairpins themselves are sufficient to allow initiation of viral DNA replication. Salvino et al. (23) studied the effects of deletions within the 5′-terminal palindrome. In plasmid clones of MVM DNA missing 9, 41, or 97 bp that encompassed the axis of symmetry in the 206-bp 5′-terminal palindrome, the MVM DNA was not excised and replicated, while MVM DNA from one mutant which lacked 82 bp from the 5′ end of the extended genome replicated only at a very low level. Nevertheless, specific elements found upstream of the right hairpin are also necessary for efficient replication (24, 25).

The 5′-terminal palindrome of MVMp can assume a hairpin structure, within the stem of which there are three unpaired nucleotides which form a bubble. Examination of the 5′ hairpin sequences of other parvoviruses, including H1 (21), LuIII (12), mink enteritis virus (15), Aleutian mink disease virus (4), porcine parvovirus (27), and the human parvovirus B19 (11) reveals, in each case, the presence of a single bubble or clusters of mismatched nucleotides. Curiously, the mismatches do not appear to occur at random throughout the length of the hairpin but are found predominantly 21 to 24 nucleotides from the terminal loop. This observation suggests that unpaired nucleotides in the 5′-terminal hairpins of these viruses play a role in their life cycles.

In this work, we measured the effects on viral DNA replication of mutating the bubble nucleotides of the MVM 5′-terminal hairpin. We provide evidence that the presence of a bubble is necessary for efficient viral DNA replication.

* Corresponding author. Phone: (21) 692-5921. Fax: (21) 652-6933.

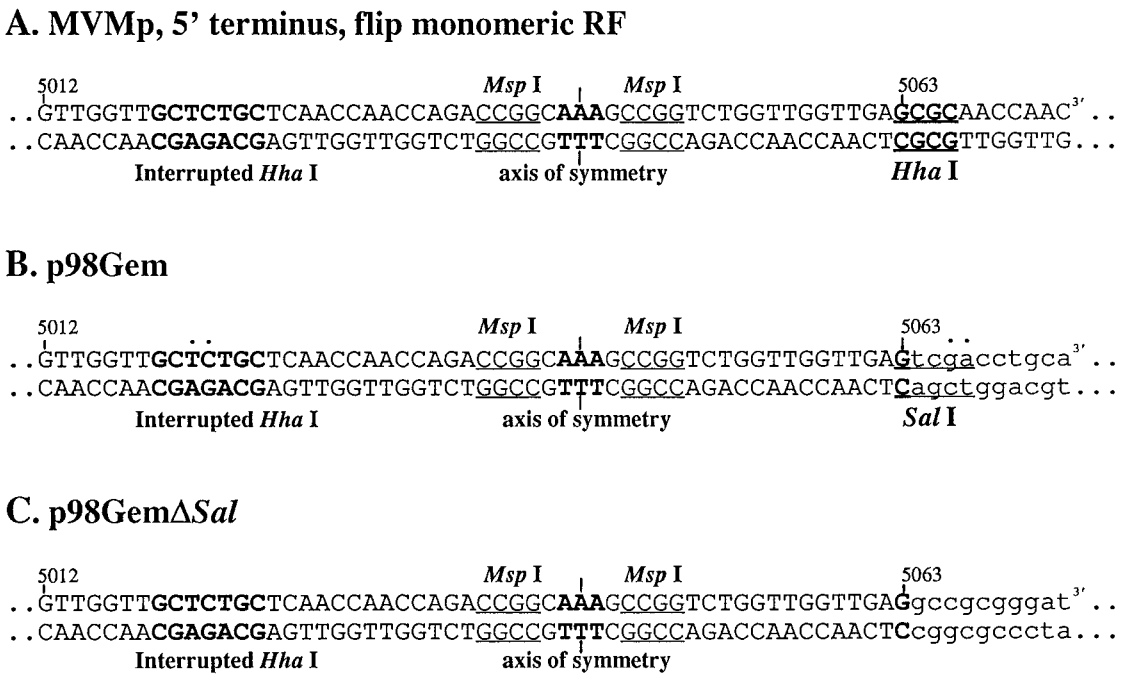

FIG. 1. Comparison of the sequence of the wild-type MVMp 5′ extended terminus with the corresponding region contained in p98Gem and p98GemΔ*Sal*. (A) Sequence of the 5′ terminus of MVMp flip mRF DNA from nucleotides 5012 to 5073. The *Hha*I site, *Msp*I sites, interrupted *Hha*I site, and axis of symmetry are indicated. (B and C) Corresponding sequence in p98Gem (B) and p98GemΔ*Sal* (C). p98Gem contains the entire sequence of MVMp up to the *Hha*I site, which has been replaced by a *Sal*I site. Plasmid vector nucleotides are represented in lowercase letters. p98GemΔ*Sal*I is identical to p98Gem except that the region containing the *Sal*I site has been removed from the pGem polylinker. The numbers indicate nucleotide positions.

MATERIALS AND METHODS

Cells and virus. A9 mouse fibroblasts were used to propagate MVM after either infection with virus or transfection with cloned mRF viral DNA. The cells were grown as monolayers in Dulbecco's modified Eagle's medium containing 5% fetal calf serum. For infection, the medium was removed from cultures that were 30 to 50% confluent and replaced by 0.4 ml of virus suspension (generally a lysate from infected cells) per 10-cm-diameter plate. After 90 min at 37°C, 10 ml of medium containing 5% fetal calf serum was added, and the infection was continued. The titers of virus stocks were estimated by plaque assay on A9 cells as described previously (16). The DNA content was compared as follows. Dilutions of virus stocks were spotted onto a nitrocellulose filter, denatured with a solution containing 0.5 M NaOH and 1.5 M NaCl for 10 min, and neutralized with a solution containing 1 M Tris (pH 7.0), 0.3 M NaCl, and 0.03 M sodium citrate for 10 min. This procedure was followed by Southern hybridization with a ^{32}P-labelled probe. The probe was synthesized by using a random prime labelling kit (Boehringer) according to the manufacturer's instructions and with p98Gem, which contains cloned MVMp mRF DNA (as described below) as the template. Alternatively, a virion DNA-specific single-stranded probe was prepared by RNA synthesis from the T7 promoter in a pGem construct which contained the full coding sequences for MVM NS-1. Signals were quantified with a PhosphorImager (Molecular Dynamics) and Image Quant software. The infectivity comparisons were based on the ratio of plaque-forming units to DNA content.

Plasmid constructs. The cloning of MVMp RF DNA into plasmid vectors was described previously (22). p98Gem contains bp 1 to 5063 of MVMp RF DNA flanked by *Sal*I linkers in pGem5Zf(+) (Promega). Thus, it contains the intact 3′ terminus and more than half of the 5′ palindrome (Fig. 1B).

p98GemΔ*Sal*I (Fig. 1C) was constructed by releasing double-stranded MVM DNA from p98Gem by digestion with *Sal*I. The *Sal*I ends were then removed by S1 nuclease digestion. This DNA was then reinserted into pGem5Zf(+) which had been linearized with *Nco*I and rendered blunt by digestion with S1 nuclease.

DNA transfections. A9 cells were transfected as described previously (19). Briefly, 10 to 20 μg of DNA (per 10-cm plate of A9 cells) was added to HEPES (*N*-2-hydroxyethylpiperazine-*N*′-2-ethanesulfonic acid)-buffered, modified Rinaldini's balanced salt solution (136 mM NaCl, 2.68 mM KCl, 0.7 mM NaH_2PO_4, 17.6 mM HEPES [pH 7.0]). $CaCl_2$ from a 2 M stock was added dropwise (to a final concentration of 0.125 M; the final volume was 1 ml), and the DNA-calcium mixture was incubated for 20 min at room temperature, during which time a fine precipitate formed. Cells were prepared by washing with phosphate-buffered saline, and fresh medium was added. The solution containing the precipitate was added to the cells and incubated for 6 h, after which time the cells were washed twice and fresh medium was added. Cells were passaged (usually two to three times) until cytopathic effect (CPE) was observed. Virus was collected by freeze-thawing the cells and subsequent centrifugation of the lysate at 800 × *g* to remove cellular debris. Plaque purification was carried out, and virus stocks made from individual plaques were used in all further procedures.

Sequence analysis of the bubble region of MVM mutants. Because of the highly palindromic nature of the 5′ terminus of MVM DNA, sequencing virion hairpin DNA is problematic. However, all the sequence information of virion hairpin DNA is contained in the 5′ termini of extended mRF DNA, which exists in two sequence orientations, termed flip and flop (2). A flip extended mRF DNA molecule differs from a flop extended mRF DNA molecule only at the axis of symmetry and points of asymmetry in the palindrome, i.e., the bubble nucleotides. Thus, by subcloning approximately half of the palindrome (and thereby eliminating the problem of sequencing hairpin DNA) of flip and flop extended mRF DNA and sequencing the region containing nucleotides involved in bubble formation (and, if necessary, the axis of symmetry), one can deduce the sequence of the viral hairpin.

Transfection of A9 cells with p98Gem and p98GemΔ*Sal* gave rise to viruses which we called MVMs and MVMx, respectively. Twenty plates of A9 cells (30% confluent) were infected with virus, and RF DNA was isolated by the method of Hirt (14). The DNA was treated with RNase (50 μg/ml) for 30 min at 37°C and then with pronase (25 μg/ml) for 30 min at the same temperature. It was extracted with phenol plus chloroform and precipitated with 2.5 volumes of ethanol. mRF DNA was digested with the restriction enzyme *Xba*I, and the 825-bp fragment corresponding to extended 5′ termini was gel purified from an 0.8% agarose gel. This fragment, which contains the bubble nucleotides and the axis of symmetry, was digested (in the case of MVMx, with limiting enzyme in order to obtain partial digests) with the restriction enzyme *Msp*I. This enzyme cuts within the terminal palindrome at nucleotides 5042 and 5051, i.e., both sides of the axis of symmetry (Fig. 1A). The *Xba*I-*Msp*I restriction fragment resulting from a complete digestion with *Msp*I lacks the axis of symmetry and thus contains slightly less than half of the 5′ palindrome. In the case of a partial *Msp*I digestion, the axis of symmetry is present; the resulting fragment thus contains slightly more than half of the palindrome. Such fragments were subcloned between the *Xba*I and *Acc*I sites of pUC19, and clones were sequenced in the *Msp*I to *Xba*I direction. The sequence of the terminal hairpin of virion DNA was deduced by comparison of the flip and flop sequences of mRF DNA.

Examination of structural differences between the 5′ hairpins of MVMx and MVMp. mRF DNA was digested with *Afl*III (see Fig. 4), and the resulting fragments were end labelled with the Klenow fragment of DNA polymerase (Boehringer) and ^{32}P-labelled dCTP. Fragments corresponding to either the 3′

terminus or the 5′ terminus (extended or hairpin) were purified from a native 12% polyacrylamide gel and subjected to restriction enzyme digestion analysis and/or resolved on a denaturing gel containing 6% acrylamide and 7 M urea. Denaturing gels were run between 60 and 64°C to prevent the formation of hairpin structures.

Mixed-infection experiments. A9 cells were infected at low multiplicity with a single type of virus or with a combination of two viruses, wild-type MVMp and either MVMs or MVMx. The ratio of wild-type to mutant virus was varied (see Results). CPE was detected after 5 days, during which time the cells were passaged (1:5) once. Virus stocks were grown by two passages in A9 cells. To determine which virus (wild type or mutant), if any, predominated after mixed infection, viral DNA was isolated and subjected to restriction enzyme analysis. The absence of the terminal *Hha*I site from the extended RF DNA of mutants MVMs and MVMx makes them distinguishable from the wild type (see Fig. 5B and C). DNA was digested with *Eco*RI, and extended 5′-terminal fragments were gel purified from an 0.8% agarose gel and digested with *Xba*I and *Hha*I. The resulting fragments were end labelled with T4 DNA polymerase and separated on a 6% polyacrylamide gel. A total of 3,000 cpm was loaded per lane. After migration, the gel was dried and autoradiographed.

Estimation of amount of accumulated replicative forms. The amount of each viral stock required to yield an equal uptake of viral single-stranded DNA into cells for MVMp, MVMs, and MVMx was estimated by infecting cells for 1.5 h, extracting viral DNA (see above), resolving it on an agarose gel, and carrying out Southern hybridization with an appropriate probe (see below). Signals were quantified with a PhosphorImager (Molecular Dynamics). Thus, A9 cells were infected with a dilution of each virus stock (MVMp, MVMs, and MVMx) so that equal DNA uptake was achieved. Virus was added to cells at 0 h, and viral DNA was harvested at 1.5, 16, 20, and 24 h. A 10-cm plate was used for each time point. One-fiftieth of the total DNA harvested from each plate was separated on a 1% Tris-acetate-EDTA-buffered agarose gel, transferred to nitrocellulose, and hybridized with a random-primed ^{32}P-labelled probe. The template for probe synthesis, p98Gem, is described above.

Examination of the ratio of 5′ hairpin to extended termini. A9 cells were infected with 0.4 ml of virus suspension, and viral DNA was isolated after 24 h as described above. Viral mRF DNA was digested with *Xba*I and separated on a 0.8% agarose gel, and the relative amounts of extended and hairpin termini for each virus were compared. The extended *Xba*I terminus has a size of 825 bp and is distinguishable from the more quickly migrating *Xba*I hairpin DNA fragment, which has a size of 705 bp (see Fig. 7B).

RESULTS

Generation of MVMs, a virus with an altered bubble in the 5′-terminal DNA hairpin. Figure 1A shows part of the sequence of 5′ flip (2) extended mRF DNA. The axis of symmetry and regions of asymmetry, namely, the *Hha*I site and the interrupted *Hha*I site, are shown in boldface. In virion DNA, nucleotides of the *Hha*I site base-pair with those of the interrupted *Hha*I site, leaving three nucleotides unpaired (which form a bubble). Thus, in order to form a wild-type bubble, the DNA sequences corresponding to both the *Hha*I site and the interrupted *Hha*I site are required. Plasmid p98Gem (see Materials and Methods) contains 5,063 bp of MVMp mRF DNA. It contains the entire 3′ end intact and extends to the last *Hha*I restriction site of the 5′ end of the flip wild-type RF DNA (Fig. 1B). It thus contains more than half of the 5′ palindrome, but since the *Hha*I site is absent, it lacks the information to form a wild-type bubble upon hairpin formation. p98Gem is an infectious clone of MVM DNA, and transfection of it into A9 fibroblasts gave rise, after plaque purification, to a virus, MVMs. Sequence analysis (Fig. 2) of extended mRF DNAs revealed that there were two distinct sequences at the location of nucleotides normally involved in bubble formation. The nucleotide sequence in Fig. 2A, left panel, is identical to the wild-type MVMp flip sequence, and we assume that it is the MVMs flip sequence. We therefore refer to the sequence in the right panel as flop.

The deduced sequence of the 5′ terminus of MVMs virion flip DNA is shown in Fig. 2B. A pair of mismatched nucleotides (GA opposite AC) in the stem of the hairpin forms a bubble. The bubble is located at the same position as the wild-type MVMp bubble (Fig. 2C); however, its sequence is altered. Apparently, neighboring plasmid sequences from the *Sal*I site of pGem (Fig. 1B, tcga, directly adjacent to nucleotide

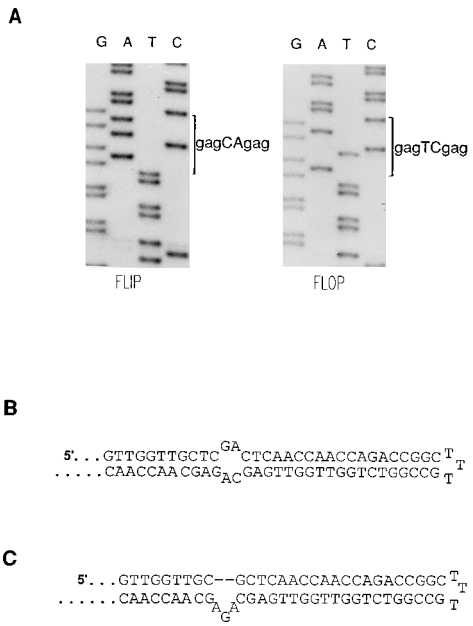

FIG. 2. Sequence analysis of the region of asymmetry in MVMs 5′ extended RF DNA. (A) Virion strand sequences involved in bubble formation are indicated by brackets for MVMs flip and flop extended mRF DNA. (B) Deduced sequence of this region of the 5′ terminus of MVMs virion DNA. (C) Corresponding sequence of MVMp hairpin DNA, flip orientation.

5063 of MVM) were incorporated into the viral DNA. This may have arisen because two of the nucleotides (ga [dotted in Fig. 1B]) can pair with nucleotides (TC [dotted in Fig. 1B]) in the interrupted *Hha*I site during hairpin formation. Sequence data and restriction analysis showed that the rest of the hairpin was like that of the wild type. This experiment was also done with the same MVM sequence (i.e., 5,063 bp of MVMp mRF DNA) flanked by *Sal*I linkers but in a different plasmid vector, pEMBL. After transfection into A9 cells, a virus identical to MVMs was obtained.

Generation of MVMx, a virus lacking a bubble in its 5′-terminal DNA hairpin. A cloned DNA (p98Gem) which lacked the sequence information to form a wild-type bubble gave rise to a virus, MVMs, which had recreated a bubble at the same position as in the wild-type virus. This implied that mismatched nucleotides may somehow be critical for growth of the virus. To examine whether a virus without a bubble at this position replicates, a new clone, p98GemΔ*Sal* (Fig. 1C), was constructed. This clone is similar to p98Gem, but the 5′-terminal *Sal*I site (part of which was used for bubble formation in MVMs) was removed. The neighboring plasmid sequence was chosen in order to avoid base-pairing with nucleotides of viral DNA upon hairpin formation. Transfection of p98GemΔ*Sal* into A9 cells gave rise, after plaque purification, to a virus, MVMx. Sequence analysis of flip and flop extended mRF DNAs showed that the two sequences were identical at the location of nucleotides which are normally involved in bubble formation (Fig. 3A), the only difference between the two sequences being the axis of symmetry, TTT for flip and AAA for flop. The deduced sequence of the 5′ terminus of MVMx virion flip DNA is shown in Fig. 3B. The AGA nucleotides, normally unpaired in the MVMp 5′ hairpin, are base-paired in the hairpin of MVMx. The bubble is thus eliminated entirely from this position.

Change in conformation of the 5′-terminal hairpin of MVMp DNA on removal of the bubble. The presence of a bubble in the

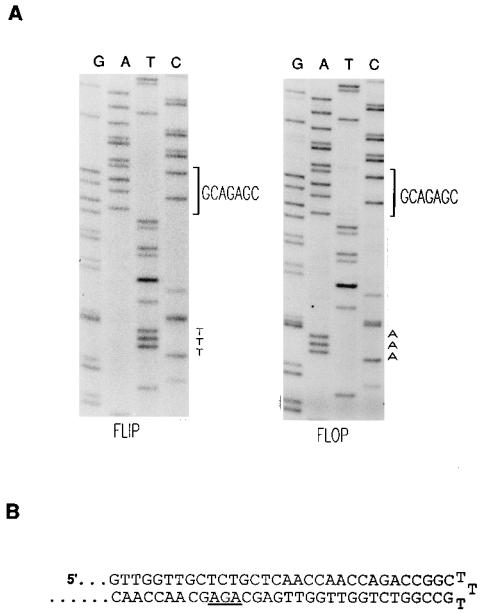

FIG. 3. Sequence analysis of the 5′ terminus of MVMx extended RF DNA. (A) Virion strand sequences involved in bubble formation (brackets) and axes of symmetry (TTT or AAA) for MVMx flip and flop extended mRF DNA. (B) Deduced DNA sequence of this region of the 5′ MVMx hairpin, flip orientation. Nucleotides that are unpaired in the wild-type hairpin are underlined.

5′-terminal hairpin of MVM is expected to cause a bend in the DNA at this position. Removal of the bubble should abolish this. In order to test this prediction, mRF DNA from MVMp and from MVMx was digested with the restriction enzyme *Afl*III, labelled with Klenow enzyme, and separated on a nondenaturing 8% polyacrylamide gel. As shown in Fig. 4A, this enzyme cuts MVM mRF DNA once in the 3′ extended terminus, at one internal site, and twice in the 5′ extended terminal palindrome; the 5′ hairpin form has a single site.

The *Afl*III DNA restriction profiles for MVMp and MVMx mRF DNA were consistently different. Figure 4B shows an example of such a profile. *Afl*III digestion of mRF DNA from MVMx gave rise to a band, X_3 (Fig. 4B, lane 2), which was not present when MVMp mRF DNA was digested (Fig. 4B, lane 1). In order to understand this discrepancy, bands P_0, P_1, P_2, X_0, X_1, X_2, and X_3 were gel purified and further analyzed. X_0 was identified as the 127-bp 5′ fragment (spanning the axis of symmetry) of MVMx by its size and the observation that heat denaturation and electrophoresis under native conditions lead to an increased mobility, corresponding to the size of hairpin DNA (data not shown). X_1 was shown by restriction analysis to be the extended 3′ restriction fragment, since it was cut with the restriction enzyme *Cfo*I but was resistant to digestion with *Rsa*I and *Msp*I (data not shown). X_2 migrated (under denaturing conditions) with a mobility corresponding to 64 nucleotides (Fig. 4C, lane 3) and was unaffected by digestion with *Rsa*I (lane 4), indicating that it is the 64-bp 5′-end fragment. X_3

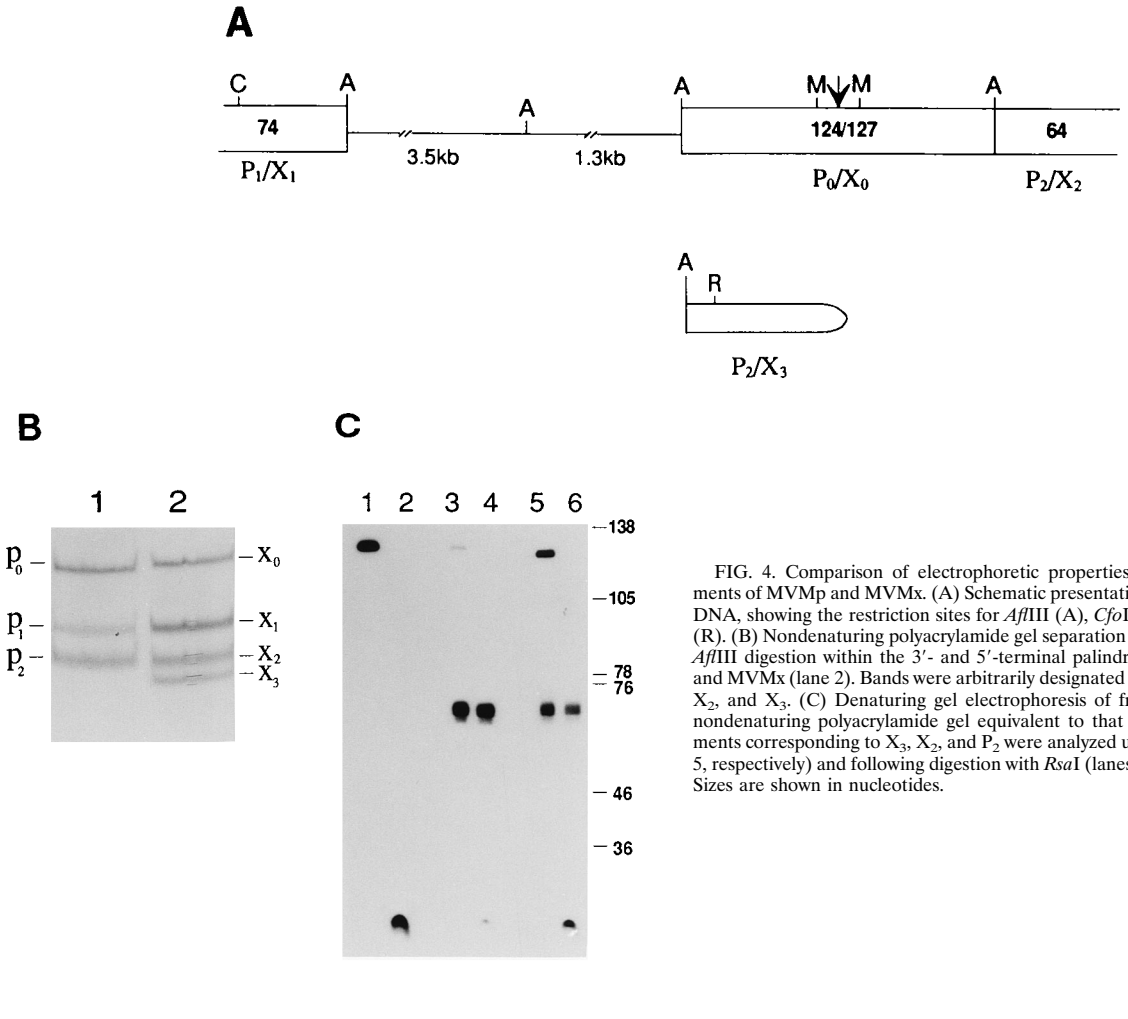

FIG. 4. Comparison of electrophoretic properties of *Afl*III terminal fragments of MVMp and MVMx. (A) Schematic presentation of extended MVM RF DNA, showing the restriction sites for *Afl*III (A), *Cfo*I (C), *Msp*I (M), and *Rsa*I (R). (B) Nondenaturing polyacrylamide gel separation of fragments arising from *Afl*III digestion within the 3′- and 5′-terminal palindromes of MVMp (lane 1) and MVMx (lane 2). Bands were arbitrarily designated P_0, P_1, and P_2 and X_0, X_1, X_2, and X_3. (C) Denaturing gel electrophoresis of fragments isolated from a nondenaturing polyacrylamide gel equivalent to that shown in panel B. Fragments corresponding to X_3, X_2, and P_2 were analyzed undigested (lanes 1, 3, and 5, respectively) and following digestion with *Rsa*I (lanes 2, 4, and 6, respectively). Sizes are shown in nucleotides.

represents the 5′ hairpin fragment of MVMx. Under denaturing conditions, it migrated with a size of 127 nucleotides (Fig. 4C, lane 1) and was cut with the restriction enzyme *Rsa*I (Fig. 4C, lane 2).

P_0, P_1, and P_2 are equivalent to X_0, X_1, and X_2, respectively, with one important exception. Under denaturing conditions, P_2 separated into two species, one of which retained the original mobility (64 nucleotides), while the other had a mobility (124 nucleotides) corresponding to denatured hairpin DNA (Fig. 4C, lane 5). Restriction with *Rsa*I (which digests within the 5′ hairpin but not in the *Afl*III extreme 5′-end fragment) resulted in loss of the band at 124 nucleotides, while the fragment of 64 nucleotides was unaffected (Fig. 4C, lane 6). This indicates that band P_2 contains two DNA species: the 5′ hairpin fragment and the 64-bp 5′-end fragment.

These results show that the 5′ hairpin DNA of MVMp migrates very differently from that of MVMx. Sequence data (Fig. 3) demonstrated that the hairpin of MVMx had three nucleotides more than that of MVMp. This was verified by their mobilities under denaturing conditions (Fig. 4C, compare lane 1 [MVMx hairpin] and the upper band in lane 5 [MVMp hairpin]). However, despite its being the shorter molecule, the wild-type hairpin migrates more slowly than that of MVMx. This is consistent with a bend or other conformation in the DNA retarding its mobility.

MVMx is outgrown by MVMp in mixed-infection experiments, whereas MVMs grows as well as the wild-type virus. The ratio of plaque-forming units to DNA content, as estimated by using a virion strand-specific probe as well as a probe which can hybridize to both strands (see Materials and Methods), was similar for MVMp and MVMs. However, that of MVMx was notably lower (35- to 75-fold in several experiments), indicating a defective virus. In order to compare the growth potential of the three different viruses, mixed-infection experiments were carried out. A9 fibroblasts were infected at low multiplicity with a single type of virus or with a combination of mutant (either MVMs or MVMx) and wild-type viruses. Cells were passaged once, at which time CPE was observed, and virus were subsequently grown by two passages in A9 cells. Extended mRF DNA was analyzed by restriction enzyme digestion (see Materials and Methods) in a manner which allowed us to distinguish between the mutants MVMx or MVMs and MVMp.

The absence of the terminal *Hha*I site from the extended RF DNA of mutants MVMs and MVMx makes them distinguishable from the wild type. This site is located 99 bp from the 5′ end of extended MVMp flip mRF DNA and 145 bp from the 5′ end of extended flop mRF DNA (Fig. 5B). Thus, digestion of an *Eco*RI 5′-terminal fragment of extended mRF DNA from MVMp with *Hha*I and *Xba*I gives two diagnostic bands of 728 and 680 bp. The absence of the *Hha*I site from MVMx and MVMs gives, in contrast, a single band of 825 bp. Infection with MVMp alone and subsequent analysis of the DNA resulted in the restriction pattern shown in Fig. 5A, lanes 2 and 6. The expected bands of 728 and 680 bp were observed. The restriction patterns observed following infection with MVMx alone or MVMs alone (Fig. 5A, lanes 1 and 5, respectively) show the diagnostic band of 825 bp. The presence of bands of 456 and 365 bp in all lanes serves as internal control, indicating that the enzyme *Hha*I was active in all samples. The restriction pattern following infection with an equal multiplicity of both MVMx and MVMp is shown in Fig. 5A, lane 3. Bands indicative of MVMp replication are predominant. Even after an initial infection in the presence of 10 times less MVMp (Fig. 5A, lane 4), MVMx was still outgrown, indicating that, compared with the wild type, MVMx is severely impaired at some point in its life cycle.

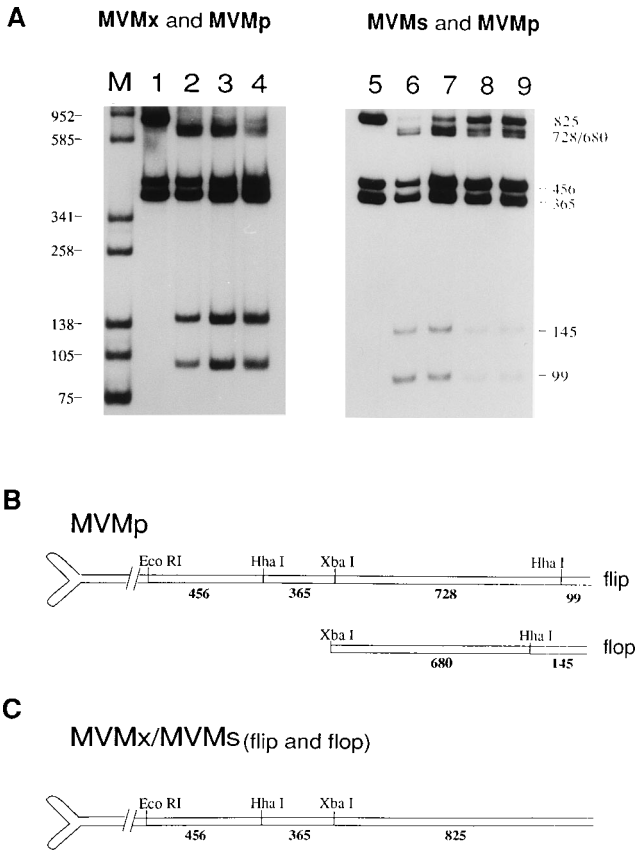

FIG. 5. (A) Agarose gel electrophoretic analysis of restriction enzyme-digested mRF DNA isolated after mixed infections. DNA was isolated from infected cells and digested with *Eco*RI, and the extended 5′-end fragments were purified and further digested with *Xba*I and *Hha*I. These fragments were then labelled and separated on a 1% agarose gel. Lanes 1 to 4 compare MVMx and MVMp restriction patterns following infection. Lanes: 1, MVMx alone (multiplicity of infection [MOI] of 0.01); 2, MVMp alone (MOI of 0.01); 3, MVMx and MVMp (both at MOIs of 0.01); 4, MVMx and MVMp (MOIs of 0.01 and 0.001, respectively). Lanes 5 to 9 compare MVMs and MVMp restriction patterns following infection. Lanes: 5, MVMs alone (MOI of 0.01); 6, MVMp alone (MOI of 0.01); 7, MVMs and MVMp (both at MOIs of 0.01); 8, MVMs and MVMp (MOIs of 0.01 and 0.002, respectively); 9, MVMs and MVMp (MOIs of 0.01 and 0.001, respectively). Molecular size markers are shown in lane M (in base pairs). (B and C) Restriction maps of 5′-terminal portions of MVMp (B) and MVMx and MVMs (C). *Eco*RI, *Xba*I, and *Hha*I sites are indicated.

When cells were infected with MVMs and MVMp at equal multiplicities, bands indicative of the presence of both viruses were observed (Fig. 5A, lane 7). After infection with 5-fold less MVMp than MVMs (Fig. 5A, lane 8) or 10-fold less MVMp than MVMs (Fig. 5A, lane 9), the predominant virus recovered was MVMs. It was not outgrown by MVMp. Thus, it is clear that MVMx and MVMs respond differently to coculture with the wild-type virus. It appears that MVMx is disadvantaged compared with MVMp during the several rounds of replication that it takes before CPE is observed. MVMs, on the other hand, grows as well as MVMp under these conditions.

MVMx accumulates replicative intermediates at a lower rate than MVMp or MVMs. Having seen that, in mixed-infection experiments, MVMx was outgrown by MVMp while MVMs was not, we examined whether the relative rate of viral DNA replication of each virus might account for this observation. A9 cells were infected with equivalent amounts (in terms

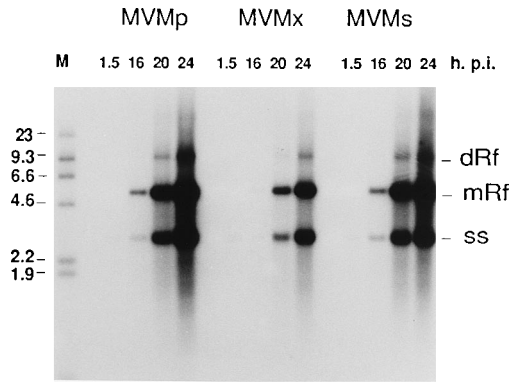

FIG. 6. Accumulation of viral replicative intermediate DNAs at various times postinfection. Cells were infected with either MVMp, MVMx, or MVMs, and the viral DNA was isolated at the indicated hours postinfection (h.p.i.) and analyzed by gel electrophoresis, transfer, and Southern hybridization. The positions of dimeric RF DNA (dRF), mRF DNA, and single strands (ss) are indicated. Lane M, molecular size markers (in kilobases).

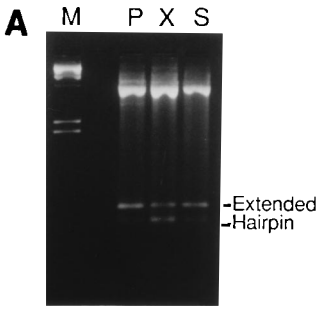

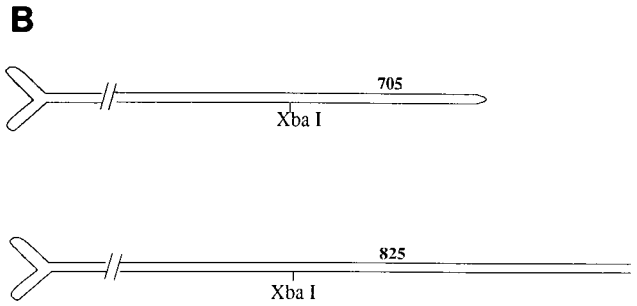

FIG. 7. Agarose gel electrophoretic analysis of *Xba*I-digested mRF DNA from MVMp (lane P), MVMx (lane X), and MVMs (lane S). The positions of fragments representing 5′ extended termini and 5′ hairpin termini are indicated. Molecular size markers are shown in lane M.

of viral DNA; see Materials and Methods) of MVMp, MVMx, or MVMs. Viral DNA was extracted at different times postinfection (1.5, 16, 20, and 24 h), and the different forms of viral DNA were detected by Southern blotting (Fig. 6). According to quantitative PhosphorImager analysis, by 16 h postinfection, mRF DNA was detected in equal amounts in cells infected with MVMp or MVMs. However, in the case of MVMx, only barely detectable levels were observed at this time. By 20 h postinfection, mRF and single-stranded DNAs were detected in extracts from cells infected with MVMx. At this time, however, almost fourfold more mRF and single-stranded DNAs were present in extracts from MVMp- or MVMs-infected cells. In fact, the profile of accumulated intermediates of DNA replication in cells infected with MVMx at 24 h postinfection resembled that of MVMp or MVMs at 20 h postinfection. Thus, replication of MVMx lagged behind that of the wild-type virus, while the virus with the altered 5′ bubble, MVMs, replicated at the same rate as the wild-type virus. This experiment was done several times with either equal amounts of virus in terms of DNA or equal numbers of plaque-forming units used for infection. MVMx was consistently seen to accumulate replication intermediates at a lower rate than MVMp or MVMs.

Altered ratio of MVMx 5′ hairpin to extended form RF DNA observed. A key step in the proposed model for MVM replication is nicking of the 5′ terminus by NS-1 and subsequent strand displacement by host cell DNA polymerase (1). This step in replication leads to conversion of the 5′ hairpin to an extended terminus. The extent to which this reaction has occurred can be assessed by digestion of mRF DNA with *Xba*I, which gives a 705-bp hairpin fragment and an 825-bp extended 5′ fragment (Fig. 7B). We isolated RF DNA at 24 h postinfection from cells infected with MVMp, MVMx, and MVMs. The ratio of extended to hairpin 5′ termini for MVM has been reported to be 9:1 (26), and we also observed this for MVMp (Fig. 7A, lane P). We detected a similar ratio for MVMs (Fig. 7A, lane S). However, in the case of MVMx, this ratio was 1:1 (Fig. 7A, lane X). Thus, it appears that the processing of the 5′ terminus of MVMx is different from that of the wild-type virus.

DISCUSSION

We have studied the effect on MVM DNA replication of the bubble in the 5′-terminal hairpin DNA of MVMp. We report that transfection of cloned MVMp DNA which lacked the sequence information to form a wild-type bubble gave rise, nonetheless, to a virus (MVMs) with a bubble at the same location as in the wild type. The sequence of the bubble was not the same as that of MVMp. Similar results were obtained when an alternative vector carrying the same DNA was used for transfection. These data indicate that a mechanism exists for the generation of a bubble and that there is a possible selection during growth for virus with a bubble.

Examination of the sequence of MVMs mRF DNA (Fig. 2A) revealed the presence of four plasmid nucleotides. We propose the following model to account for this. The process of excision of MVM DNA is not fully understood but may involve NS-1-mediated nicking (20) and displacement synthesis through the palindrome. In our experiments, the viral protein NS-1 is encoded by the transfected DNA. In a way analogous to that proposed for MVM DNA replication (1), the newly made strand would dissociate and fold into a hairpin. Nucleotides which can base-pair are retained as part of the hairpin. Those which cannot are excised by a cellular repair mechanism. The four plasmid nucleotides (5′-tcga-3′) are retained because of the base-pairing of two of them (ga) with MVM nucleotides in the hairpin. The stability of this base-pairing and the capacity of these two nucleotides to serve as a primer for extention by DNA polymerase will be critical in determining whether they too are retained. If not, the formation of a variety of viruses with different arrangements of bubble nucleotides is possible. If the bubble serves a useful function for MVM, then the virus(es) with the optimum sequence in this region will have an advantage over the others and will be selected.

We show that a virus lacking a bubble was less infectious and replicated less well than the wild-type virus. These data imply

that, for efficient replication, the virus requires an intact bubble. Alteration in the sequence of nucleotides of the bubble did not affect viral function. The behavior of MVMs was, in every respect examined, identical to that of wild-type MVMp. This is perhaps not surprising, since in nature the sequence of nucleotides involved in bubble formation is different in the so-called flip and flop forms. Thus, it would appear that the presence of a bubble rather than the actual sequence of nucleotides at that position is important. Many other parvoviruses have mismatched or unpaired nucleotides in their 5′-terminal hairpins. The sequence of these bubbles is not conserved, but interestingly, their position in the hairpin appears to be. The MVM hairpin is 100 bp in length, with a single bubble located 20 bp away from the first unpaired base of the terminal loop. The positioning of the mismatches around a region 21 to 24 nucleotides from the end of the hairpin has been seen in other parvoviruses examined (see the introduction). The absence of unpaired nucleotides elsewhere in these molecules is notable and is true even in the case of very long hairpins, e.g., that of the human parvovirus B19. An exception is bovine parvovirus, which does not have mismatches in the 42-bp stem of its 5′-terminal hairpin (5). However, the terminal loop of bovine parvovirus has 13 nucleotides unpaired, compared with the smaller, more commonly found terminal loops containing three unpaired nucleotides, of MVM, Aleutian mink disease virus G, H1, porcine parvovirus, LuIII, and mink enteritis virus. The large single stranded loop of bovine parvovirus may somehow compensate for the lack of neighboring mismatches. The stem of the adeno-associated virus hairpin also lacks mismatches, but the hairpin itself can assume a T-shaped structure quite unlike those of the viruses mentioned above and may therefore have different requirements for replication.

What is the function of the mismatched nucleotides in the 5′ hairpin of MVM? A role in DNA replication is evident. According to current models of MVM DNA replication (1), an early step in the process involves NS-1-mediated site-specific nicking at the 5′ terminus. Recently, Cotmore et al. (6) have identified a binding site, $(ACCA)_{2-3}$, for NS-1. Such a site (AC CAACCA) occurs on each side of the bubble, very close to it. There are also putative NS-1 binding sites on either side of the 5′ nick site. Nicking by NS-1 is followed by opening of the hairpin and synthesis of a new strand, using the original palindrome as the template, resulting in extended mRF DNA. In MVMx, the ratio of hairpin to extended 5′ termini is disproportionately high, indicating diminished processing of this hairpin during replication. This result may be due to an inability of NS-1 to operate efficiently in the absence of a bubble. Alternatively, elimination of the bubble may have caused the removal of a denaturation nucleation site and thus hindered the process of displacement synthesis. It must be remembered, however, that the bubble is some 98 bp from the point at which displacement begins.

It is possible that for efficient nicking, the interaction of factors other than NS-1 with the DNA and/or each other is required. Cotmore and Tattersall (10) demonstrated that spacing of nucleotides within the replication origin at the 3′ end of the MVM genome is critical for replication initiation. The generation of MVMx involved the introduction of three extra nucleotides into the hairpin. Altered spacing in the hairpin may have been responsible for the failure of MVMx to replicate as efficiently as the wild type. We generated a virus, MVMz, in which the nucleotides which form the bubble were deleted (as opposed to complemented in the case of MVMx), thus shortening rather than lengthening the hairpin. Like MVMx, this bubbleless mutant exhibited a low ratio of plaque-forming units to DNA and was defective in the accumulation of replicative intermediates.

The active replication origin at the 3′ end of MVM DNA is a stretch of perfectly base-paired duplex DNA approximately 50 nucleotides long (10). By contrast, the origin of replication at the 5′ terminus is part of a hairpin in which secondary structure may play a role. We demonstrate a physical consequence of the presence of the bubble. Comparison of the hairpins of MVMp and MVMx showed that the presence of unpaired nucleotides caused a decrease in mobility on a polyacrylamide gel. This is indicative of different secondary structures and may reflect a bend in the 5′-terminal DNA hairpin of MVMp. Secondary structure has been shown to influence the interaction of the Rep protein (whose function in the replication of adeno-associated virus is analogous to that of NS-1 in MVM replication) with its DNA recognition sequence. While Rep can bind to a linear duplex segment of the adeno-associated virus terminal repeat, it binds with higher affinity to the complete terminal repeat in hairpin form (18). It is possible that the alteration in conformation of the MVMx hairpin may account for the defects in replication of the viral DNA. Although NS-1 site-specific DNA binding has been detected (6), it is likely that it functions in association with accessory proteins. Loss of the bubble and its associated conformation may have led to a less effective interaction of such proteins (or of NS-1 itself) with the hairpin.

ACKNOWLEDGMENTS

We are grateful to K. Willwand for providing the p98Gem plasmid and to B. Bentele for excellent technical assistance.

This work was supported by the Swiss National Science Foundation and Swiss Cancer League.

REFERENCES

1. **Astell, C. R., M. B. Chow, and D. C. Ward.** 1985. Sequence analysis of the termini of virion and replicative forms of minute virus of mice DNA suggests a modified rolling hairpin model for autonomous parvovirus DNA replication. J. Virol. **54:**171–177.
2. **Astell, C. R., M. Thomson, M. Merchlinsky, and D. C. Ward.** 1983. The complete DNA sequence of minute virus of mice, an autonomous parvovirus. Nucleic Acids Res. **11:**999–1018.
3. **Berns, K. I.** 1990. Parvovirus replication. Microbiol. Rev. **54:**316–329.
4. **Bloom, M. E., S. Alexandersen, C. F. Garon, S. Mori, W. Wei, S. Perryman, and J. B. Wolfinbarger.** 1990. Nucleotide sequence of the 5′-terminal palindrome of Aleutian mink disease parvovirus and construction of an infectious molecular clone. J. Virol. **64:**3551–3556.
5. **Chen, K. C., B. C. Shull, M. Lederman, E. R. Stout, and R. C. Bates.** 1988. Analysis of the termini of the DNA of bovine parvovirus: demonstration of sequence inversion at the left terminus and its implication for the replication model. J. Virol. **62:**3807–3813.
6. **Cotmore, S. F., J. Christensen, J. P. Nuesch, and P. Tattersall.** 1995. The NS1 polypeptide of the murine parvovirus minute virus of mice binds to DNA sequences containing the motif $[ACCA]_{2-3}$. J. Virol. **69:**1652–1660.
7. **Cotmore, S. F., J. P. Nuesch, and P. Tattersall.** 1992. In vitro excision and replication of 5′ telomeres of minute virus of mice DNA from cloned palindromic concatemer junctions. Virology **190:**365–377.
8. **Cotmore, S. F., J. P. Nuesch, and P. Tattersall.** 1993. Asymmetric resolution of a parvovirus palindrome in vitro. J. Virol. **67:**1579–1589.
9. **Cotmore, S. F., and P. Tattersall.** 1992. In vivo resolution of circular plasmids containing concatemer junction fragments from minute virus of mice DNA and their subsequent replication as linear molecules. J. Virol. **66:**420–431.
10. **Cotmore, S. F., and P. Tattersall.** 1994. An asymmetric nucleotide in the parvoviral 3′ hairpin directs segregation of a single active origin of DNA replication. EMBO J. **13:**4145–4152.
11. **Deiss, V., J. D. Tratschin, M. Weitz, and G. Siegl.** 1990. Cloning of the human parvovirus B19 genome and structural analysis of its palindromic termini. Virology **175:**247–254.
12. **Diffoot, N., B. C. Shull, K. C. Chen, E. R. Stout, M. Lederman, and R. C. Bates.** 1989. Identical ends are not required for the equal encapsidation of plus- and minus-strand parvovirus LuIII DNA. J. Virol. **63:**3180–3184.
13. **Faust, E. A., and D. C. Ward.** 1979. Incomplete genomes of the parvovirus minute virus of mice: selective conservation of genome termini, including the origin for DNA replication. J. Virol. **32:**276–292.

14. **Hirt, B.** 1967. Selective extraction of polyoma DNA from infected mouse cell cultures. J. Mol. Biol. **26:**365–369.
15. **Kariatsumari, T., M. Horiuchi, E. Hama, K. Yaguchi, N. Ishigurio, H. Goto, and M. Shinagawa.** 1991. Construction and nucleotide sequence analysis of an infectious DNA clone of the autonomous parvovirus, mink enteritis virus. J. Gen. Virol. **72:**867–875.
16. **Kimsey, P. B., H. D. Engers, B. Hirt, and C. V. Jongeneel.** 1986. Pathogenicity of fibroblast- and lymphocyte-specific variants of minute virus of mice. J. Virol. **59:**8–13.
17. **Liu, Q., C. B. Yong, and C. R. Astell.** 1994. In vitro resolution of the dimer bridge of the minute virus of mice (MVM) genome supports the modified rolling hairpin model for MVM replication. Virology **201:**251–262.
18. **McCarty, D. M., J. H. Ryan, S. Zolotukhin, X. Zhou, and N. Muzyczka.** 1994. Interaction of the adeno-associated virus Rep protein with a sequence within the A palindrome of the viral terminal repeat. J. Virol. **68:**4998–5006.
19. **Potter, K. N., and L. K. Miller.** 1980. Transfection of two invertebrate cell lines with DNA of Autographa californica nuclear polyhedrosis virus. J. Invertebr. Pathol. **36:**431–432. (Abstract.)
20. **Rhode, S. L., III.** 1989. Both excision and replication of cloned autonomous parvovirus DNA require the NS1 (Rep) protein. J. Virol. **63:**4249–4256.
21. **Rhode, S. L., III, and B. Klaassen.** 1982. DNA sequence of the 5′ terminus containing the replication origin of parvovirus replicative form DNA. J. Virol. **41:**990–999.
22. **Sahli, R.** 1985. Etude moléculaire d'un variant immunosuppressif de MVM, un parvovirus murin. Ph.D. thesis, University of Lausanne, Lausanne, Switzerland.
23. **Salvino, R., M. Skiadopoulos, E. A. Faust, P. Tam, R. O. Shade, and C. R. Astell.** 1991. Two spatially distinct genetic elements constitute a bipartite DNA replication origin in the minute virus of mice genome. J. Virol. **65:** 1352–1363.
24. **Tam, P., and C. R. Astell.** 1993. Replication of minute virus of mice minigenomes: novel replication elements required for MVM DNA replication. Virology **193:**812–824.
25. **Tam, P., and C. R. Astell.** 1994. Multiple cellular factors bind to *cis*-regulatory elements found inboard of the 5′ palindrome of minute virus of mice. J. Virol. **68:**2840–2848.
26. **Tullis, G., R. V. Schoborg, and D. J. Pintel.** 1994. Characterization of the temporal accumulation of minute virus of mice replicative intermediates. J. Gen. Virol. **75:**1633–1646.
27. **Vasudevacharya, J., S. Basak, R. V. Srinivas, and R. W. Compans.** 1990. The complete nucleotide sequence of an infectious clone of porcine parvovirus, strain NADL-2. Virology **178:**611–616.